Enterococcus faecalis CRISPR-Cas is a robust barrier to conjugative antibiotic resistance dissemination in the murine intestine

Valerie J. Price[a], Sara W. McBride[b], Karthik Hullahalli[a], Anushila Chatterjee[b], Breck A. Duerkop[b#], and Kelli L. Palmer[a#]

Department of Biological Sciences, The University of Texas at Dallas, Richardson, Texas, USA[a]

Department of Immunology & Microbiology, The University of Colorado School of Medicine, Aurora, Colorado, USA[b]

Running head: CRISPR-Cas anti-plasmid activity *in vitro* and *in vivo*

#Address correspondence to breck.duerkop@ucdenver.edu (BAD) or kelli.palmer@utdallas.edu (KLP)

Abstract

CRISPR-Cas systems are barriers to horizontal gene transfer (HGT) in bacteria. Little is known about CRISPR-Cas interactions with conjugative plasmids, and studies investigating CRISPR-Cas/plasmid interactions in *in vivo* models relevant to infectious disease are lacking. These are significant gaps in knowledge because conjugative plasmids disseminate antibiotic resistance genes among pathogens *in vivo*, and it is essential to identify strategies to reduce the spread of these elements. We use enterococci as models to understand the interactions of CRISPR-Cas with conjugative plasmids. *Enterococcus faecalis* is a native colonizer of the mammalian intestine and harbors pheromone-responsive plasmids (PRPs). PRPs mediate inter- and intraspecies transfer of antibiotic resistance genes. We assessed *E. faecalis* CRISPR-Cas anti-PRP activity in the mouse intestine and under varying *in vitro* conditions. We observed striking differences in CRISPR-Cas efficiency *in vitro* versus *in vivo*. With few exceptions, CRISPR-Cas blocked intestinal PRP dissemination, while *in vitro*, the PRP frequently escaped CRISPR-Cas defense. Our results further the understanding of CRISPR-Cas biology by demonstrating that standard *in vitro* experiments do not adequately model the *in vivo* anti-plasmid activity of CRISPR-Cas. Additionally, our work identifies several variables that impact the apparent *in vitro* anti-plasmid activity of CRISPR-Cas, including planktonic versus biofilm settings, different donor/recipient ratios, production of a plasmid-encoded bacteriocin, and the time point at which matings are sampled. Our results are clinically significant because they demonstrate that barriers to HGT encoded by normal human microbiota can have significant impacts on *in vivo* antibiotic resistance dissemination.

39 **Importance**

40 CRISPR-Cas is a type of immune system encoded by bacteria that is hypothesized to
41 be a natural impediment to the spread of antibiotic resistance genes. In this study, we
42 directly assessed the impact of CRISPR-Cas on antibiotic resistance dissemination in
43 the mammalian intestine and under varying *in vitro* conditions. We observed a robust
44 effect of CRISPR-Cas on *in vivo* but not *in vitro* dissemination of antibiotic resistance
45 plasmids in the native mammalian intestinal colonizer *Enterococcus faecalis*. We
46 conclude that standard laboratory experiments currently do not appropriately model the
47 *in vivo* conditions where antibiotic resistance dissemination occurs between *E. faecalis*
48 strains. Moreover, our results demonstrate that CRISPR-Cas encoded by native
49 members of the mammalian intestinal microbiota can block the spread of antibiotic
50 resistance plasmids.

51

52

53 **Introduction**

54 CRISPR-Cas systems confer adaptive immunity against mobile genetic elements
55 (MGEs) in bacteria (1-3). CRISPR-Cas systems utilize nucleases programmed with
56 small RNAs to direct sequence-specific cleavage of nucleic acids including phage and
57 plasmids (4). Most experimental studies of native CRISPR-Cas systems have examined
58 either anti-phage defense or defense against electrotransformed plasmids in low
59 complexity *in vitro* systems. Comparatively little information is available on the roles of
60 CRISPR-Cas in regulating plasmid conjugation, and there have been few experimental
61 studies assessing the function of CRISPR-Cas systems within the native ecology of
62 microbial communities. These are major weaknesses in the field from a public health
63 perspective. Conjugative plasmids disseminate antibiotic resistance genes, and
64 CRISPR-Cas systems are naturally occurring barriers that could impede the
65 dissemination of these genes in mammalian microbiota.

66

67 We use *Enterococcus faecalis* as a model organism to study the interactions of
68 CRISPR-Cas systems with conjugative plasmids. *E. faecalis* is a gram-positive
69 bacterium, a native inhabitant of the mammalian intestine (5), and an opportunistic
70 pathogen that is among the leading causes of hospital-acquired infections (HAIs) in the
71 United States (6, 7). *E. faecalis* strains causing HAIs possess unique characteristics
72 relative to strains that normally colonize the human intestine. HAI strains typically have
73 larger genomes resulting from rampant plasmid, phage, and other MGE acquisition (8,
74 9). Multidrug-resistant (MDR) *E. faecalis* generally lack CRISPR-Cas systems, and
75 there is a correlation between the absence of CRISPR-Cas and the presence of

76 horizontally acquired antibiotic resistance in *E. faecalis* clinical isolates (10). From
77 genomic analyses, it appears that CRISPR-Cas is a potent barrier to the horizontal
78 acquisition of antibiotic resistance in *E. faecalis*. Our subsequent efforts have attempted
79 to experimentally address this hypothesis.
80
81 The model plasmids we use for our studies are the pheromone-responsive plasmids
82 (PRPs). The PRPs appear to be highly co-evolved with *E. faecalis* (11, 12). PRPs are
83 large (can be >60 kb) and encode accessory traits such as antibiotic resistance,
84 bacteriocin production, reduced UV light susceptibility, and enhanced biofilm formation
85 (11). PRPs encoding antibiotic resistance genes are often present in *E. faecalis*
86 infection isolates (11, 13-15). The model PRP, pAD1, encodes genes for production and
87 self-immunity to a bacteriocin called cytolysin (16). Cytolysin is a lantibiotic-like
88 antimicrobial peptide and hemolysin with activity against a number of gram-positive
89 bacteria (17, 18).
90
91 In this study, we utilize *E. faecalis* T11RF, a non-MDR strain that encodes a Type II
92 CRISPR-Cas system referred to as CRISPR3-Cas (10, 19). Type II CRISPR-Cas
93 systems employ a Cas9-crRNA-tracrRNA ribonucleoprotein complex to generate
94 double-stranded DNA breaks in invading MGEs (3, 20, 21). Sequence specificity in the
95 cleavage event is conferred by the crRNA (22). A crRNA is encoded by a short
96 sequence referred to as a spacer, which is derived from and is complementary to a
97 previously encountered MGE (1, 23, 24). The *E. faecalis* T11RF CRISPR3-Cas system
98 encodes a spacer with perfect sequence complementarity to the *repB* gene of the PRP

99 pAD1 (10, 19). In previous studies, we demonstrated that the *E. faecalis* CRISPR3-Cas
100 system interferes with the conjugative acquisition of pAM714 (19), a pAD1 variant with
101 an insertion of Tn*917* encoding *ermB* (25, 26). More specifically, pAM714 acquisition is
102 decreased by ~80-fold in *E. faecalis* T11RF relative to T11RF∆*cas9* after 18 hours
103 biofilm mating on an agar surface, and CRISPR3-Cas defense against pAM714 requires
104 the targeting spacer (19). These results support our overarching hypothesis that
105 CRISPR-Cas is a significant barrier to the horizontal acquisition of antibiotic resistance
106 in *E. faecalis*. However, the magnitude of CRISPR3-Cas impact on pAM714 acquisition,
107 while significant, was low compared with the overall high transfer rate of pAM714 under
108 the conditions tested. Many pAM714 molecules escaped CRISPR3-Cas defense
109 despite T11RF possessing functional CRISPR-Cas. We have made similar observations
110 in other *E. faecalis* strains using both native and engineered CRISPR-Cas systems and
111 with both naturally occurring and engineered plasmids (19, 27, 28). We previously
112 defined the ability of cells to acquire CRISPR-targeted plasmids at high frequencies as
113 CRISPR tolerance (27).
114
115 To investigate potential explanations for the seeming discrepancy between the
116 presence of CRISPR-Cas in wild *E. faecalis* isolates and our *in vitro* observations of
117 statistically significant but middling population-level impact of CRISPR-Cas on
118 conjugative plasmid transfer, we first assessed whether different *in vitro* mating
119 conditions alter conclusions reached about CRISPR-Cas defense efficiency. We
120 compared pAM714 acquisition by wild type and ∆*cas9* T11RF recipients in planktonic
121 and agar plate biofilm matings using time course experiments and two different initial

122 donor/recipient ratios. We performed the same experiments with the PRP pAM771,
123 which is a pAD1 derivative possessing a Tn*917* insertion in the cytolysin locus (25, 29,
124 30). We reasoned that killing of plasmid-free recipient cells by the cytolysin could
125 'punish' cells that utilize CRISPR-Cas against the plasmid, potentially altering the
126 apparent efficacy of CRISPR-Cas. We also assessed the transfer of pAM714 and
127 pAM771 to wild-type and Δ*cas9* T11RF recipients in a murine intestinal colonization
128 model. To our knowledge, this is the first study to assess the impact of CRISPR-Cas on
129 conjugative antibiotic resistance dissemination in a mammalian intestinal model. We
130 discovered that CRISPR-Cas is a strikingly robust barrier to pAM714 and pAM771
131 acquisition in the murine intestine.
132
133 **Results**
134 **Mating conditions impact CRISPR-Cas activity against pAM714.** We analyzed
135 planktonic and agar plate mating reactions between *E. faecalis* OG1SSp(pAM714)
136 donors and T11RF or T11RF Δ*cas9* recipients over an 18-hour period (Fig. 1; see Table
137 1 for strain details). We inoculated mating reactions at donor to recipient ratios of 1:9
138 and 1:1 (Fig. 1). Donors were quantified by plating matings on media with
139 spectinomycin, streptomycin, and erythromycin (Fig. S1); transconjugants with
140 rifampicin, fusidic acid, and erythromycin (Fig. 1), and total recipients (which includes
141 transconjugants) with rifampicin and fusidic acid (Fig. 2-3). In our experiments, we used
142 erythromycin resistance to track pAM714 conjugation. *ermB* is encoded on Tn*917*,
143 which theoretically could transpose from pAM714 into the *E. faecalis* chromosome,
144 thereby unlinking erythromycin resistance from pAM714 presence. However, Tn*917*

145 transposition frequencies are very low (10^{-6}) in the absence of the inducer erythromycin
146 (31). No mating reactions in our study contained erythromycin.
147
148 For 1:9 donor:recipient ratio experiments, we observed ~10^3-10^4 transconjugants for
149 both T11RF and Δ*cas9* recipients after 30 minutes of mating (Fig. 1A-B).
150 T11Δ*cas9*(pAM714) transconjugant numbers remained stable for the remainder of the
151 planktonic mating experiment, while T11RF(pAM714) transconjugant numbers
152 decreased (Fig. 1A). In contrast, pAM714 transconjugant yields in biofilm matings rose
153 over time for both T11RF and Δ*cas9* recipients, up to the 2 hour time point. After that,
154 T11RF(pAM714) transconjugant numbers did not increase further, while
155 T11Δ*cas9*(pAM714) transconjugants increased by 2 log (Fig. 1B). For both planktonic
156 and biofilm matings, we observed significant differences in transconjugant yields
157 between T11RF and Δ*cas9* recipients at the experiment end point (18 hours) and for
158 some earlier time points. We note that, despite CRISPR-Cas activity, ~10^5 pAM714
159 transconjugants were still observed for T11RF recipients in biofilms (Fig. 1B).
160
161 We next assessed conjugation using an equal (1:1) donor:recipient ratio. Increasing
162 donor densities relative to recipients reduces pheromone detection by pheromone-
163 responsive plasmids (32). Transconjugant numbers were overall lower than those
164 observed for 1:9 ratio experiments (Fig. 1C-D). For planktonic matings, transconjugant
165 numbers were at or below our limit of detection, therefore the impact of *cas9* on
166 transconjugant yield could not be assessed (Fig. 1C). Transconjugants were detected
167 for biofilm matings (Fig. 1D), but the yields were lower than those observed for 1:9 ratio

168 experiments (Fig. 1B). Nevertheless, *cas9* protected recipients from pAM714 acquisition
169 at the 5 and 18 h time points (Fig. 1D).
170
171 **Cytolysin activity depletes recipient cells irrespective of functional CRISPR-Cas.**
172 We hypothesized that the cytolysin encoded by pAM714 could kill recipient cells that
173 utilize CRISPR-Cas against the plasmid. pAM771 is isogenic with pAM714, except that
174 the Tn*917* insertion disrupts *cylL* of the cytolysin biosynthesis gene cluster (25, 29, 30).
175 pAM714 and pAM771 have been utilized in previous studies assessing the impact of
176 cytolysin on virulence, hamster intestinal colonization, and plasmid transfer (29, 30, 33).
177 We performed planktonic and biofilm mating reactions with OG1SSp(pAM771) donors
178 and compared the results with the OG1SSp(pAM714) mating experiments.
179
180 Recipient (Fig. 2-3) but not donor (Fig. S1-S2) densities were substantially impacted in
181 all pAM714 mating reactions, irrespective of *cas9* presence or absence. The effect was
182 stronger in planktonic matings (Fig. 2A-B and Fig. 3A-B) than in biofilm matings (Fig.
183 2C-D and Fig. 3C-D), and strongest in planktonic matings at a 1:1 donor:recipient ratio,
184 where recipient numbers fell to below the limit of detection after 1.5 h of mating (Fig. 3A-
185 B). These results are consistent with pAM714 transconjugant yields under these
186 conditions (Fig. 1C). In biofilm matings, striking effects on recipient cell densities were
187 not observed until later time points (5 h and 18 h; Fig. 2C-D and Fig. 3C-D).
188
189 Unlike observations from pAM714 matings, recipient numbers were stably high in
190 pAM771 matings. Moreover, pAM771 transconjugant yields were not substantially

191 impacted by donor:recipient ratio (Fig. 4). Similar transconjugant yields were detected
192 for planktonic matings at 1:9 (Fig. 4A) and 1:1 (Fig. 4C) ratios, and for biofilm matings at
193 the two ratios (Fig. 4B and Fig. 4D, respectively). The effect of *cas9* was minor in
194 magnitude but statistically significant at the end of planktonic mating. Deletion of *cas9*
195 increased plasmid acquisition significantly, by ~2 log, after 18 h of biofilm mating.
196
197 Our results overall with *in vitro* experiments demonstrate that planktonic versus biofilm
198 settings, different donor/recipient ratios, production of a plasmid-encoded bacteriocin,
199 and the time points at which matings are sampled all impact transconjugant yields and
200 conclusions reached about the apparent activity of CRISPR-Cas. Moreover, CRISPR
201 tolerance is consistently observed *in vitro*, with the exception of settings where little
202 plasmid transfer occurs into any recipient (pAM714 planktonic matings at a 1:1
203 donor:recipient ratio; Fig. 1C).
204
205 ***cas9* expression in T11RF biofilms and planktonic cultures.** Little is known about
206 the transcriptional or post-transcriptional regulation of *cas9* in *E. faecalis*. During our
207 investigation of a different Type II CRISPR-Cas system in *E. faecalis*, CRISPR1-Cas,
208 we observed that 27-fold overexpression of *cas9* enhanced *in vitro* defense against
209 PRP-mobilizable plasmids by ~2-3 logs (27). Because low *cas9* expression in wild-type
210 T11RF under *in vitro* conditions could impact CRISPR-Cas defense, we attempted to
211 assess T11RF *cas9* expression levels under these conditions.
212

213 We first assessed T11RF *cas9* expression in monoculture under the same planktonic
214 and biofilm conditions used for mating (Fig. 5). We normalized to *recA* because this was
215 the normalization used for our previous assessment of engineered *cas9* expression in a
216 different *E. faecalis* strain (27). We observed very low expression of *cas9* relative to
217 *recA* in the early biofilm time points, and a dramatic increase in this ratio at the 5 and 18
218 hour time points (Fig. 5B). While this is consistent with the impact of *cas9* on
219 transconjugant yields in biofilm mating experiments (Fig. 1 and Fig. 4), an important
220 caveat is that we noted substantially lower *recA* expression at 5 h and 18 h in biofilm
221 T11RF cultures relative to earlier time points (Dataset S1), and thus *cas9* levels may be
222 under represented at these later time points. For planktonic cultures, relative *cas9*
223 expression levels varied in the mid-range between the high and low extremes observed
224 during biofilm growth (Fig. 5A). This, too, is consistent with transconjugant yields
225 observed in planktonic settings, where a robust effect of *cas9* was not observed for
226 pAM771 matings (Fig. 4), and in pAM714 matings the killing of recipient cells was a
227 major confounder (Fig. 2-3). We did not observe the same variation over time in *recA*
228 expression in planktonic cultures as we did for biofilm cultures (Dataset S1). Overall, the
229 relative expression of *cas9* to *recA* is consistent with *cas9* impact on transconjugant
230 yields, but the mechanism for this is unclear.
231
232 **CRISPR-Cas is a robust barrier to PRP acquisition in the murine intestine.** We
233 assessed CRISPR3-Cas activity against pAM714 and pAM771 in a mouse model of *E.*
234 *faecalis* intestinal dysbiosis. To establish antibiotic-induced dysbiosis, mice were
235 administered a cocktail of antibiotics in their drinking water for seven days, followed by

236 placement on regular water for 24 h. The mice were colonized sequentially with
237 recipient and donor *E. faecalis* strains at a 1:1 donor:recipient ratio. Fecal pellets were
238 collected at 24, 48, and 96 hours post co-colonization, homogenized, and the number of
239 transconjugants, donors, and recipients were quantified (Fig. 6). Experimental groups
240 consisting of different combinations of donor and recipient strains were used: OG1SSp
241 with T11RF as a plasmid-free control group, OG1SSp(pAM714) donors with T11RF
242 recipients, and OG1SSp(pAM714) donors with T11RF∆*cas9* recipients. In separate
243 experiments, OG1SSp(pAM771) donors were used.
244
245 We detected pAM714 transconjugants in only one of fourteen mice colonized with
246 T11RF recipients at 24 h post co-colonization, and for none of the mice at 48 and 96 h
247 time points (Fig 6A). Strikingly, pAM714 transconjugants at densities up to ~5 x 10^6
248 CFU/g of feces were observed for twelve of fourteen mice colonized with T11RF∆*cas9*
249 recipients over the course of the experiment (Fig. 6A). We screened 36 presumptive
250 T11RF∆*cas9*(pAM714) transconjugants by PCR amplification of the pAM714 *repB*
251 gene; all possessed this gene (Fig. S3). We observed that some control (no plasmid)
252 mice at 48 and 96 h time points had colony growth on media with selection for
253 transconjugants (i.e. media supplemented with rifampicin, fusidic acid, and
254 erythromycin) (Fig. 6A). We screened 20 of these colonies by PCR amplification of the
255 pAM714 *repB* gene; none possessed this gene (Fig. S3). We infer that recipients
256 received erythromycin resistance determinants from the native mouse microbiota via a
257 non-pAM714-dependent mechanism.
258

259 We performed identical *in vivo* conjugation experiments with OG1SSp(pAM771) donors.
260 Fewer mice were observed with sporadic erythromycin resistance in the control group
261 for pAM771 experiments (Fig. 6B). T11RF(pAM771) transconjugants were detected for
262 only one of ten mice at each of the 24 and 48 h time points, whereas
263 T11RF∆*cas9*(pAM771) transconjugants were detected in all eleven mice and at all time
264 points (Fig. 6B).
265
266 Overall, these data demonstrate that there is a profound impact of CRISPR-Cas on
267 plasmid transfer between *E. faecalis* strains in the dysbiotic mouse intestine. These
268 observations are in contrast to any *in vitro* condition evaluated, where either plasmid
269 transfer was not observed (for 1:1 ratio planktonic matings) or transconjugants arose
270 despite recipients having CRISPR-Cas defense. Moreover, cytolysin did not impact *in*
271 *vivo* plasmid transfer, as was observed for *in vitro* transfer. This is consistent with a
272 previous study that analyzed transfer of pAM714 and pAM771 between *E. faecalis* in
273 the hamster intestinal tract (29).
274
275 **Potential cytolysin-independent *in vivo* colonization benefit to strains possessing**
276 **a PRP.** We next assessed whether cytolysin impacted the colonization of *E. faecalis*
277 donors in the mouse intestine. We compared donor densities in control mice colonized
278 with OG1SSp to those colonized with OG1SSp(pAM714) (Fig. 6C) or
279 OG1SSp(pAM771) (Fig. 6D). We observed no benefit to donors possessing pAM714
280 versus pAM771. However, donor densities in the control group were significantly
281 reduced compared to plasmid-bearing donors at all time points. These data suggest that

282 there is a cytolysin-independent colonization benefit for OG1SSp harboring pAM714 or
283 pAM771. This is consistent with recent observations for *E. faecalis* harboring the PRP
284 pCF10 during intestinal colonization of germ-free mice (34).
285
286 At 24 hours post-co-colonization, recipient strain densities from control, pAM714, and
287 pAM771 test groups were similar (Fig. 6E-F). On average, T11RF recipient densities
288 increased in control mice at subsequent time points, but decreased in both pAM714 and
289 pAM771 test groups (Fig. 6E-F). No differences were observed for recipient densities in
290 pAM714 versus pAM771 groups. This demonstrates that the reduction in recipient cell
291 densities observed *in vitro* for pAM714 but not pAM771 matings (Fig. 2-3) does not
292 occur in the *in vivo* model tested here. Rather, our data suggest that there is a cytolysin-
293 independent fitness advantage for pAM714/pAM771 donors *in vivo*. We also note that
294 no differences were observed in T11RF and T11RF∆*cas9* colonization, indicating that
295 the presence or absence of *cas9* does not impact intestinal colonization success in this
296 model (Fig. 6E-F).
297
298 **Discussion**
299
300 We have found that native CRISPR-Cas encoded by a member of the mammalian
301 intestinal microbiota can block the *in vivo* dissemination of an antibiotic resistance
302 plasmid in a murine intestinal colonization model. This is in contrast to *in vitro*
303 observations, where the same plasmid is frequently acquired by recipient cells despite
304 CRISPR-Cas. For the *E. faecalis* CRISPR1-Cas system we previously investigated (27,

305 28), these tolerant cells harboring both CRISPR-Cas and a plasmid it targets have an *in*
306 *vitro* growth defect that is resolved by either plasmid loss or by mutation of CRISPR-Cas
307 when antibiotic selection for the plasmid is applied. We did not detect CRISPR tolerance
308 *in vivo*. One possible explanation for this is that CRISPR-Cas is far more effective *in*
309 *vivo* than *in vitro*, and transconjugants never arise in cells possessing functional
310 CRISPR-Cas *in vivo*. Another is that they do arise, but their growth defect combined
311 with turnover of intestinal contents results in their rapid elimination *in vivo*. One method
312 to test this would be to add erythromycin selection *in vivo*; we would expect to observe
313 high densities of T11RF plasmid transconjugants that are CRISPR-Cas mutants. We
314 were not able to test this in our current model system because of the erythromycin
315 inducibility of Tn*917*, which would complicate plasmid detection.
316
317 What mechanisms underlie our observations about the impact of CRISPR-Cas on
318 conjugative plasmid transfer *in vitro* and *in vivo*? Several factors may factor in this
319 process, including plasmid host range, donor to recipient ratios and their relative
320 colonization densities, community spatial structure (i.e. biofilms), flow and dilution rate,
321 nutrient availability, community diversity and the relative densities of plasmid-
322 susceptible versus non-susceptible hosts, and selection for the plasmid. With the PRPs,
323 there is the additional consideration of pheromone concentration; the pheromone is a
324 short peptide elaborated by recipient *E. faecalis* cells (and some other bacteria) that
325 induces transcription of conjugation genes in the donor strain (11, 12). Finally, there are
326 CRISPR-Cas-specific factors about which little is known, such as the *in vitro* versus *in*
327 *vivo* transcriptional and post-transcriptional regulation of *cas9*.

328

329 We confirmed that several of these factors influence PRP transconjugant yield *in vitro*.
330 *In vitro cas9* expression appears to be insufficient to confer protection to many *E.*
331 *faecalis* recipients. Other factors having strong effects were cytolysin biosynthesis
332 encoded by the plasmid, which negatively impacted recipient densities, and the
333 donor:recipient ratio, which affects induction of conjugation by pheromone signaling
334 (32).

335

336 We determined that the pAM714/pAM771 conjugation frequency to T11RF∆*cas9*
337 recipients is ~10^{0}-10^{-2} transconjugants per donor (TC/D) for *in vitro* broth and agar plate
338 biofilm experiments, while *in vivo* it ranges from 10^{-3} to 10^{-7} (Fig. S4). Conjugation
339 frequency of PRPs can be modulated by deleting aggregation substance in the plasmid,
340 which should reduce conjugation frequency in broth cultures but not biofilms (11), or by
341 interfering with pheromone production by plasmid-free recipient cells. This will be
342 addressed in future work. Also to be addressed is the effect of varying the total cell
343 count of the donors and recipients at the time of culture inoculation; initiating cultures
344 with fewer cells may more accurately reflect the nature of intestinal colonization by *E.*
345 *faecalis*.

346

347 In the *in vivo* model used here, we induced intestinal dysbiosis with antibiotics, allowed
348 mice to recover for one day, and then colonized them with *E. faecalis*. This models what
349 can occur in patients after receiving antibiotic therapy. Another mouse model used in
350 the field establishes long-term colonization of *E. faecalis* without major disruption of

351 normal intestinal microbiota (35). Further, a recent study utilized a germ-free mouse
352 model to examine *in vivo* transfer of the PRP pCF10 among intestinal *E. faecalis* (34). In
353 the germ-free model, enterococci achieve very high densities and diversity is very low.
354 In the native colonization model, diversity is high, and production of the Bac-21
355 bacteriocin from the PRP pPD1 significantly enhances *E. faecalis* colonization (35).
356 These two models can be used to assess how community diversity and the densities of
357 plasmid-susceptible and non-susceptible hosts impact CRISPR-Cas efficacy *in vivo*.
358
359 How far can we extrapolate from studies with *E. faecalis* to other members of the
360 mammalian microbiota, and from PRPs to other plasmids with different properties and
361 host ranges? Put another way, does CRISPR-Cas encoded by other members of the
362 native microbiota confer the same robust defense against antibiotic resistance plasmids
363 as observed for *E. faecalis* and PRPs? Will *E. faecalis* CRISPR-Cas defense against
364 non-PRP plasmids be equally robust? Much future work remains to elucidate these
365 questions.
366

367 **Materials and Methods**

368

369 **Bacteria and reagents used.** Strains used in this study are shown in Table 1. *E.*
370 *faecalis* strains were cultured in brain heart infusion (BHI) broth or on BHI agar at 37°C.
371 Antibiotic concentrations used were as follows: rifampicin, 50 µg/mL; fusidic acid, 25
372 µg/mL; spectinomycin, 500 µg/mL; streptomycin, 500 µg/mL; erythromycin, 50 µg/mL.

373 Antibiotics were purchased from Sigma-Aldrich or Research Products International
374 (RPI).
375
376 **Conjugation experiments.** Donor and recipient strains were cultured overnight in BHI
377 broth in the absence of antibiotic selection. The following day, cultures were diluted 1:10
378 into fresh BHI and incubated at 37°C for 1.5 hours. For planktonic conjugations at a 1:9
379 donor:recipient ratio, 2 mL of donor and 18 mL of recipient were mixed in a flask and
380 incubated without agitation at 37°C for 30 min to 18 h. For planktonic conjugations at a
381 1:1 donor:recipient ratio, 10 mL of donor and 10 mL of recipient were mixed in a flask
382 and incubated without agitation at 37°C for 30 min to 18 h. At each time point, 1 mL of
383 the mating reaction was removed and used for serial dilutions and plating on selective
384 media. For biofilm mating reactions at a 1:9 donor:recipient ratio, 100 µL of donor was
385 mixed with 900 µL of recipient, and for reactions at a 1:1 donor:recipient ratio, 500 µL of
386 donor was mixed with 500 µL of recipient. The mixture was centrifuged for 1 min at
387 16,000 x g. After centrifugation, 100 µL supernatant was used to resuspend the pellet,
388 which was then spread-plated on non-selective BHI agar. To allow for sampling of
389 multiple time points of biofilms, multiple identical conjugation reactions were generated
390 using the same donor and recipient inocula. The conjugation reactions were incubated
391 at 37°C for 30 min to 18 h. At each time point, cells were collected by washing and
392 scraping an agar plate using 2 mL 1X phosphate buffered saline (PBS) supplemented
393 with 2 mM EDTA, and serial dilutions were plated on selective media. For all matings,
394 BHI agar supplemented with antibiotics was used to quantify the donor (spectinomycin,
395 streptomycin, and erythromycin), recipient (rifampicin and fusidic acid), and

396 transconjugant (rifampicin, fusidic acid, and erythromycin) populations. Plates were
397 incubated for 36-48 h at 37°C. Plates with 30 to 300 colonies were used to calculate
398 CFU/mL.
399
400 **Mouse model of *E. faecalis* colonization.** Seven days prior to bacterial colonization,
401 6-8 week old C57BL/6 mice were gavaged with 100 µL of an antibiotic cocktail
402 (streptomycin 1 mg/mL, gentamicin 1 mg/mL, erythromycin 200 µg/mL), and given a
403 water bottle ad libitum with the same antibiotic cocktail for 6 days following gavage. 24 h
404 prior to bacterial inoculation, antibiotic water was removed and replaced with standard
405 sterile antibiotic-free water. Bacteria were grown overnight in BHI, and mice were
406 gavaged with 10^9 CFU in PBS of each bacterial strain as experimental groups indicated
407 (1:1 donor:recipient ratio). Samples used for gavage were plated on BHI to confirm that
408 inocula were equal across strains. Fecal samples from mice were collected at 0 h, 24 h,
409 48 h and 96 h. Fecal samples were resuspended in 1 mL of sterile PBS and dilutions
410 were plated on BHI agar supplemented with antibiotics to quantify the donor
411 (spectinomycin, streptomycin, and erythromycin), recipient (rifampicin and fusidic acid),
412 and transconjugant (rifampicin, fusidic acid, and erythromycin) populations. Plates were
413 incubated for 36-48 h at 37°C. Plates with 30 to 300 colonies were used to calculate
414 CFU/g of feces. Experiments were performed in duplicate or triplicate as follows: For
415 OG1SSp pAM714/T11RF(+/- *cas9*) co-colonization, three independent experiments
416 were performed consisting of 4, 4, and 6 mice per group per experiment. For OG1SSp
417 pAM771/T11RF(+/- *cas9*) co-colonization, two independent experiments were
418 performed consisting of 5 mice per group, except in the second experiment where 5

419 mice were used for the control and wild-type T11RF groups and 6 mice were used for
420 the T11RF Δ*cas9* group. Data from individual experimental replicates were combined
421 and graphed together. All animal protocols were approved by the Institutional Animal
422 Care and Use Committee of the University of Colorado Anschutz Medical Campus
423 (protocol number 00253).
424
425 **Colony PCR to verify *in vivo* transconjugants.** Fecal pellets were collected at 0 hr,
426 24 hr, 48 hr and 96 hr, weighed, and resuspended in 1 mL PBS. 20 µL were plated at
427 multiple dilutions on BHI containing rifampicin, fusidic acid, and erythromycin. Individual
428 colonies were picked, resuspended in 20 µL nuclease-free water, and 1 µL used in PCR
429 with Taq DNA Polymerase (New England Biolabs). Primers amplified the *repB* region of
430 plasmids pAM714 and pAM771 (pAD1 *repB*-For: 5'-CGT TCC ATG TGT CTA ACA ATT
431 GTA TTA AAC-3' and pAD1 *repB*-Rev: 5'-CGA TGA TGG TAG CAA TTC AAG AAG G-
432 3').
433
434 ***In vitro* T11RF *cas9* expression analysis.** Identical growth conditions and procedures
435 were used as described above for planktonic and biofilm conjugation experiments with
436 the exception that the OG1SSp plasmid donor strain was not present. At the desired
437 time point, a 5 mL culture aliquot was collected from planktonic cultures conditions, or
438 biofilms were collected from agar plates using 2 mL of PBS supplemented with 2 mM
439 EDTA. Total RNA was isolated using RNA-Bee and chloroform precipitation as
440 previously described (36). 200 ng RNA was used as template for cDNA synthesis using
441 qScript cDNA Supermix (Quanta Biosiences). Subsequent qPCR reactions were

442 performed using the AzuraQuant Green Fast qPCR Mix LoRox (Azura Genomics).
443 Primer sequences to query *cas9* were *cas9*-For: 5'-GCA ACT GGG ATG ACT ATC A-3'
444 and *cas9*-Rev: 5'-GCA TAA CGC GTA TCA TTC A-3'. Primer sequences to query *recA*
445 were *recA*-For: 5'-TGG TGA GAT GGG AGC GAG CC-3' and *recA*-Rev: 5'-TCA GGA
446 TTT CCG AAC ATC ACG CC-3'. Expression of *cas9* relative to *recA* was calculated as
447 2ΔCq, where ΔCq = (CqT11RF @ time x *cas9* – CqT11RF @ time x *recA*). Data shown
448 represents the average *cas9* expression from three independent experiments for both
449 growth conditions assessed.
450

451 **Acknowledgments**

452 The authors thank Ian Jorgeson with assistance with figure formatting and Dr. Michael
453 Gilmore for providing pAM714 and pAM771. This work was supported by grants
454 R01AI116610 to KLP, R01AI141479 to BAD, and K01DK102436 to BAD from the
455 National Institutes of Health. The authors declare that the funders of this work had no
456 role in the design of experiments, interpretation of data, or the decision to publish this
457 work.
458

459 **References Cited**
460

461 1. **Barrangou R, Fremaux C, Deveau H, Richards M, Boyaval P, Moineau S,**
462 **Romero DA, Horvath P.** 2007. CRISPR provides acquired resistance against
463 viruses in prokaryotes. Science **315:**1709-1712.
464 2. **Marraffini LA, Sontheimer EJ.** 2008. CRISPR interference limits horizontal
465 gene transfer in staphylococci by targeting DNA. Science **322:**1843-1845.
466 3. **Garneau JE, Dupuis ME, Villion M, Romero DA, Barrangou R, Boyaval P,**
467 **Fremaux C, Horvath P, Magadan AH, Moineau S.** 2010. The CRISPR/Cas
468 bacterial immune system cleaves bacteriophage and plasmid DNA. Nature
469 **468:**67-71.
470 4. **Barrangou R, Horvath P.** 2017. A decade of discovery: CRISPR functions and
471 applications. Nat Microbiol **2:**17092.
472 5. **Lebreton F, Willems RJL, Gilmore MS.** 2014. Enterococcus Diversity, Origins
473 in Nature, and Gut Colonization. *In* Gilmore MS, Clewell DB, Ike Y, Shankar N
474 (ed.), Enterococci: From Commensals to Leading Causes of Drug Resistant
475 Infection, Boston.
476 6. **Lake JG, Weiner LM, Milstone AM, Saiman L, Magill SS, See I.** 2018.
477 Pathogen Distribution and Antimicrobial Resistance Among Pediatric Healthcare-
478 Associated Infections Reported to the National Healthcare Safety Network, 2011-
479 2014. Infection Control and Hospital Epidemiology **39:**1-11.
480 7. **Weiner LM, Webb AK, Limbago B, Dudeck MA, Patel J, Kallen AJ, Edwards**
481 **JR, Sievert DM.** 2016. Antimicrobial-Resistant Pathogens Associated With
482 Healthcare-Associated Infections: Summary of Data Reported to the National

483 Healthcare Safety Network at the Centers for Disease Control and Prevention,
484 2011-2014. Infection Control and Hospital Epidemiology **37:**1288-1301.
485 8. **Palmer KL, Godfrey P, Griggs A, Kos VN, Zucker J, Desjardins C, Cerqueira**
486 **G, Gevers D, Walker S, Wortman J, Feldgarden M, Haas B, Birren B,**
487 **Gilmore MS.** 2012. Comparative genomics of enterococci: variation in
488 *Enterococcus faecalis*, clade structure in *E. faecium*, and defining characteristics
489 of *E. gallinarum* and *E. casseliflavus*. MBio **3:**e00318-00311.
490 9. **Van Tyne D, Manson AL, Huycke MM, Karanicolas J, Earl AM, Gilmore MS.**
491 2019. Impact of antibiotic treatment and host innate immune pressure on
492 enterococcal adaptation in the human bloodstream. Sci Transl Med **11**.
493 10. **Palmer KL, Gilmore MS.** 2010. Multidrug-resistant enterococci lack CRISPR-
494 *cas*. MBio **1**: e00227-10.
495 11. **Clewell DB, Weaver KE, Dunny GM, Coque TM, Francia MV, Hayes F.** 2014.
496 Extrachromosomal and Mobile Elements in Enterococci: Transmission,
497 Maintenance, and Epidemiology. *In* Gilmore MS, Clewell DB, Ike Y, Shankar N
498 (ed.), Enterococci: From Commensals to Leading Causes of Drug Resistant
499 Infection, Boston.
500 12. **Dunny GM.** 2013. Enterococcal sex pheromones: signaling, social behavior, and
501 evolution. Annual Review of Genetics **47:**457-482.
502 13. **Wardal E, Gawryszewska I, Hryniewicz W, Sadowy E.** 2013. Abundance and
503 diversity of plasmid-associated genes among clinical isolates of *Enterococcus*
504 *faecalis*. Plasmid **70:**329-342.

505 14. **Mikalsen T, Pedersen T, Willems R, Coque TM, Werner G, Sadowy E, van**
506 **Schaik W, Jensen LB, Sundsfjord A, Hegstad K.** 2015. Investigating the
507 mobilome in clinically important lineages of *Enterococcus faecium* and
508 *Enterococcus faecalis*. BMC Genomics **16:**282.
509 15. **Freitas AR, Novais C, Tedim AP, Francia MV, Baquero F, Peixe L, Coque**
510 **TM.** 2013. Microevolutionary events involving narrow host plasmids influences
511 local fixation of vancomycin-resistance in *Enterococcus* populations. PloS ONE
512 **8:**e60589.
513 16. **Clewell DB.** 2007. Properties of *Enterococcus faecalis* plasmid pAD1, a member
514 of a widely disseminated family of pheromone-responding, conjugative, virulence
515 elements encoding cytolysin. Plasmid **58:**205-227.
516 17. **Booth MC, Bogie CP, Sahl HG, Siezen RJ, Hatter KL, Gilmore MS.** 1996.
517 Structural analysis and proteolytic activation of *Enterococcus faecalis* cytolysin, a
518 novel lantibiotic. Mol Microbiol **21:**1175-1184.
519 18. **Cox CR, Coburn PS, Gilmore MS.** 2005. Enterococcal cytolysin: a novel two
520 component peptide system that serves as a bacterial defense against eukaryotic
521 and prokaryotic cells. Curr Protein Pept Sci **6:**77-84.
522 19. **Price VJ, Huo W, Sharifi A, Palmer KL.** 2016. CRISPR-Cas and Restriction-
523 Modification Act Additively against Conjugative Antibiotic Resistance Plasmid
524 Transfer in *Enterococcus faecalis*. mSphere **1:**e00064-00016.
525 20. **Gasiunas G, Barrangou R, Horvath P, Siksnys V.** 2012. Cas9-crRNA
526 ribonucleoprotein complex mediates specific DNA cleavage for adaptive

527 immunity in bacteria. Proceedings of the National Academy of Sciences
528 **109:**E2579-2586.
529 21. **Jinek M, Chylinski K, Fonfara I, Hauer M, Doudna JA, Charpentier E.** 2012. A
530 programmable dual-RNA-guided DNA endonuclease in adaptive bacterial
531 immunity. Science **337:**816-821.
532 22. **Brouns SJ, Jore MM, Lundgren M, Westra ER, Slijkhuis RJ, Snijders AP,**
533 **Dickman MJ, Makarova KS, Koonin EV, van der Oost J.** 2008. Small CRISPR
534 RNAs guide antiviral defense in prokaryotes. Science **321:**960-964.
535 23. **Jansen R, van Embden JD, Gaastra W, Schouls LM.** 2002. Identification of a
536 novel family of sequence repeats among prokaryotes. Omics **6:**23-33.
537 24. **Bolotin A, Quinquis B, Sorokin A, Ehrlich SD.** 2005. Clustered regularly
538 interspaced short palindrome repeats (CRISPRs) have spacers of
539 extrachromosomal origin. Microbiology **151:**2551-2561.
540 25. **Ike Y, Clewell DB, Segarra RA, Gilmore MS.** 1990. Genetic analysis of the
541 pAD1 hemolysin/bacteriocin determinant in *Enterococcus faecalis*: Tn*917*
542 insertional mutagenesis and cloning. Journal of Bacteriology **172:**155-163.
543 26. **Clewell DB, Tomich PK, Gawron-Burke MC, Franke AE, Yagi Y, An FY.** 1982.
544 Mapping of *Streptococcus faecalis* plasmids pAD1 and pAD2 and studies relating
545 to transposition of Tn*917*. Journal of Bacteriology **152:**1220-1230.
546 27. **Hullahalli K, Rodrigues M, Nguyen UT, Palmer K.** 2018. An Attenuated
547 CRISPR-Cas System in *Enterococcus faecalis* Permits DNA Acquisition. MBio **9**:
548 e00414-18.

549 28. **Hullahalli K, Rodrigues M, Palmer KL.** 2017. Exploiting CRISPR-Cas to
550 manipulate *Enterococcus faecalis* populations. Elife **6**: e26664.
551 29. **Huycke MM, Gilmore MS, Jett BD, Booth JL.** 1992. Transfer of pheromone-
552 inducible plasmids between *Enterococcus faecalis* in the Syrian hamster
553 gastrointestinal tract. Journal of Infectious Diseases **166:**1188-1191.
554 30. **Jett BD, Jensen HG, Nordquist RE, Gilmore MS.** 1992. Contribution of the
555 pAD1-encoded cytolysin to the severity of experimental *Enterococcus faecalis*
556 endophthalmitis. Infect Immun **60:**2445-2452.
557 31. **Tomich PK, An FY, Clewell DB.** 1980. Properties of erythromycin-inducible
558 transposon Tn*917* in *Streptococcus faecalis*. Journal of Bacteriology **141:**1366-
559 1374.
560 32. **Bandyopadhyay A, O'Brien S, Frank KL, Dunny GM, Hu WS.** 2016.
561 Antagonistic Donor Density Effect Conserved in Multiple Enterococcal
562 Conjugative Plasmids. Applied and Environmental Microbiology **82:**4537-4545.
563 33. **Cox CR, Gilmore MS.** 2007. Native microbial colonization of Drosophila
564 melanogaster and its use as a model of *Enterococcus faecalis* pathogenesis.
565 Infect Immun **75:**1565-1576.
566 34. **Hirt H, Greenwood-Quaintance KE, Karau MJ, Till LM, Kashyap PC, Patel R,**
567 **Dunny GM.** 2018. *Enterococcus faecalis* Sex Pheromone cCF10 Enhances
568 Conjugative Plasmid Transfer *In Vivo*. mBio **9:**e00037-00018.
569 35. **Kommineni S, Bretl DJ, Lam V, Chakraborty R, Hayward M, Simpson P, Cao**
570 **Y, Bousounis P, Kristich CJ, Salzman NH.** 2015. Bacteriocin production

571 augments niche competition by enterococci in the mammalian gastrointestinal
572 tract. Nature **526:**719-722.
573 36. **Huo W, Adams HM, Zhang MQ, Palmer KL.** 2015. Genome Modification in
574 *Enterococcus faecalis* OG1RF Assessed by Bisulfite Sequencing and Single-
575 Molecule Real-Time Sequencing. Journal of Bacteriology **197:**1939-1951.
576 37. **McBride SM, Fischetti VA, Leblanc DJ, Moellering RC, Jr., Gilmore MS.**
577 2007. Genetic diversity among *Enterococcus faecalis*. PloS ONE **2:**e582.
578

579 **Figure legends**

580

581 **Figure 1. Impact of CRISPR-Cas on pAM714 transconjugant yields under different**
582 ***in vitro* conditions.** The CFU/mL of transconjugants obtained in mating reactions
583 sampled over an 18-hour period is shown for T11RF (squares) and T11RF∆*cas9*
584 (triangles) recipient strains. Conjugation was performed under planktonic conditions in
585 broth (A and C) and biofilm conditions on an agar plate (B and D) utilizing OG1SSp as a
586 donor strain. Conjugation reactions were initiated with a 1:9 (A and B) or 1:1 (C and D)
587 donor to recipient ratio. The limit of detection is indicated by the dashed line. Data
588 shown are the average and standard deviation from a minimum of three independent
589 trials for each time point. Statistical significance was assessed using a two-tailed
590 Student's t-Test; *P*-values, *<0.05, **<0.01 and ***<0.001.

591

592 **Figure 2. Recipient cell densities for *in vitro* conjugations at a 1:9 donor to**
593 **recipient ratio.** T11RF (squares) and T11RF∆*cas9* (triangles) recipient cell densities in
594 CFU/mL was determined for both planktonic (A and B) and biofilm (C and D) mating
595 reactions with pAM714 (open, red symbols) and pAM771 (closed green symbols)
596 donors. The limit of detection was 10^2 CFU/mL. Data shown are the average and
597 standard deviation from a minimum of three independent trials for each time point for
598 both mating conditions. Statistical significance was assessed using a two-tailed
599 Student's t-Test; *P*-values, *<0.05, **<0.01 and ***<0.001.

600

601 **Figure 3. Recipient cell densities for *in vitro* conjugations at a 1:1 donor to**
602 **recipient ratio.** T11RF (squares) and T11RF∆*cas9* (triangles) recipient cell densities in
603 CFU/mL was determined for both planktonic (A and B) and biofilm (C and D) mating
604 reactions with pAM714 (open, red symbols) and pAM771 (closed green symbols)
605 donors. The limit of detection is indicated by the dashed line. Data shown are the
606 average and standard deviation from a minimum of three independent trials for each
607 time point for both mating conditions. Statistical significance was assessed using a two-
608 tailed Student's t-Test; *P*-values, *<0.05, **<0.01 and ***<0.001.
609
610 **Figure 4. Impact of CRISPR-Cas on pAM771 transconjugant yields under different**
611 ***in vitro* conditions.** The CFU/mL of transconjugants obtained in mating reactions
612 sampled over an 18-hour period is shown for T11RF (squares) and T11RF∆*cas9*
613 (triangles) recipient strains. Conjugation was performed under planktonic conditions in
614 broth (A and C) and biofilm conditions on an agar plate (B and D) utilizing OG1SSp as a
615 donor strain. Conjugation reactions were initiated with a 1:9 (A and B) or 1:1 (C and D)
616 donor to recipient ratio. The limit of detection is indicated by the dashed line. Data
617 shown are the average and standard deviation from a minimum of three independent
618 trials for each time point. Statistical significance was assessed using a two-tailed
619 Student's t-Test; *P*-values, *<0.05, **<0.01 and ***<0.001.
620
621 **Figure 5. T11RF *cas9* expression in planktonic culture and agar plate biofilms.**
622 Expression of *cas9* was assessed by RT-qPCR under identical growth conditions used
623 for planktonic (A) and biofilm (B) conjugation experiments, with the exception that the

624 OG1SSp plasmid donor strain was not present. Expression of *cas9* is expressed
625 relative to *recA*. Data shown represent the average *cas9* expression from three
626 independent experiments.
627
628 **Figure 6. Impact of CRISPR-Cas on plasmid transfer in the mouse intestine.** The
629 number of transconjugant (A, B), donor (C, D), and recipient (E, F) CFU/g of feces for
630 individual mice were determined by plating feces on selective agars. Each symbol
631 represents one mouse. Experimental groups are described in the materials and
632 methods. Black horizontal bars represent the geometric mean of data in each group.
633 Shown are data for *in vivo* pAM714 (A, C, and E; open red symbols) pAM771 (B, D, and
634 F; closed green symbols) transfer. Control mice co-colonized by OG1SSp and T11RF
635 are represented by open circles. Mice colonized with T11RF recipients are represented
636 by squares. Mice colonized with T11RF∆*cas9* recipients are represented by triangles.
637 The limit of detection is indicated by the dashed line. Statistical significance was
638 assessed using a two-tailed Student's t-Test; *P*-value, **<0.01 and ***<0.001.
639
640 **Supplemental figure legends**
641
642 **Figure S1. Donor cell densities for *in vitro* conjugations at a 1:9 donor to recipient**
643 **ratio.** T11RF (squares) and T11RF∆*cas9* (triangles) donor cell densities in CFU/mL was
644 determined for both planktonic (A and B) and biofilm (C and D) mating reactions with
645 pAM714 (open, red symbols) and pAM771 (closed green symbols) donors. The limit of
646 detection was 10^2 CFU/mL. Data shown are the average and standard deviation from a

647 minimum of three independent trials for each time point for both mating conditions.
648 Statistical significance was assessed using a two-tailed Student's t-Test; *P*-values,
649 *<0.05, **<0.01 and ***<0.001.
650
651 **Figure S2. Donor cell densities for *in vitro* conjugations at a 1:1 donor to recipient**
652 **ratio.** T11RF (squares) and T11RF∆*cas9* (triangles) donor cell densities in CFU/mL was
653 determined for both planktonic (A and B) and biofilm (C and D) mating reactions with
654 pAM714 (open, red symbols) and pAM771 (closed green symbols) donors. The limit of
655 detection was 10^2 CFU/mL. Data shown are the average and standard deviation from a
656 minimum of three independent trials for each time point for both mating conditions.
657 Statistical significance was assessed using a two-tailed Student's t-Test; *P*-values,
658 *<0.05, **<0.01 and ***<0.001.
659
660 **Figure S3. PCR confirms that experimental transconjugants carry pAM714 and**
661 **spontaneous resistant isolates from control animals do not.** Agarose gels show
662 PCR amplification products for the *repB* gene of pAM714 at 24 (A), 48 (B) and 96 (C)
663 hours post-colonization, and the lack of a *repB* amplification signal in isolates originating
664 from control mice and growing on transconjugant selection agar (B and D). PCR
665 reactions for the presence and absence of the *repB* gene using strains
666 OG1SSp(pAM714), OG1SSp, T11RF and T11RF ∆*cas9* are included on each gel. Rif –
667 Rifampicin, Fus – Fusidic acid, Erm – Erythromycin.
668

669 **Figure S4. Frequency of conjugation *in vitro* and in the mouse intestine.**
670 Conjugation frequencies for pAM714 under mouse intestine (A), planktonic (C), and
671 biofilm (E) settings are shown as transconjugants per donor. Conjugation frequencies
672 for pAM771 under mouse intestine (B), planktonic (D), and biofilm (F) settings are also
673 shown. Experiments with T11RF recipients are represented with squares; with T11RF
674 Δ*cas9* recipients as triangles. For calculating *in vivo* conjugation frequencies, the
675 conjugation frequency for each mouse was determined by dividing the transconjugant
676 CFU/g by the donor CFU/g; one symbol represents one mouse on the graph. Black
677 horizontal bars represent the geometric mean of data in each group. No symbol means
678 that a frequency could not be calculated because one or both of the values (donor
679 CFU/g or transconjugant CFU/g) were zero. Statistical significance was assessed using
680 a two-tailed Student's t-Test; *P*-values, *<0.05, **<0.01 and ***<0.001.
681
682

683 **Table 1. *E. faecalis* strains used in this study.**

Strain Name	Description	Reference
T11RF	Rifampicin-fusidic acid resistant derivative of strain T11	(19, 37)
T11RF∆*cas9*	T11RF with an in-frame deletion of *cas9*	(19)
OG1SSp(pAM714)	Spectinomycin-streptomycin resistant derivative of strain OG1 harboring pAM714, conferring erythromycin resistance via Tn*917* insertion upstream of the *par* locus; *cyl*$^{+}$	(25, 26)
OG1SSp(pAM771)	Spectinomycin-streptomycin resistant derivative of strain OG1 harboring pAM771, conferring erythromycin resistance via Tn*917* insertion disrupting *cylL* of the cytolysin operon; *cyl*$^{-}$	(25, 29, 30)

684

685

Figure 1

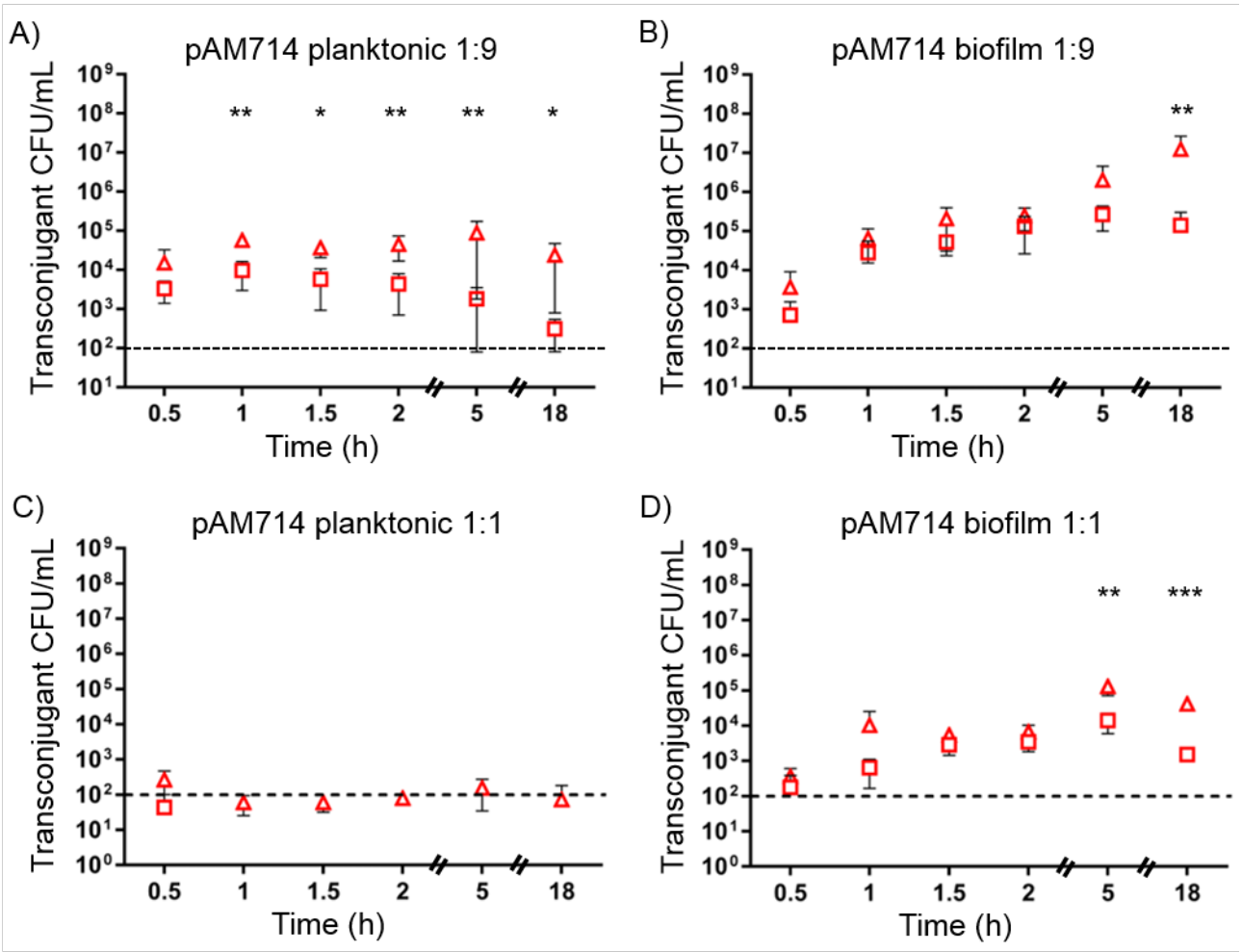
A)
pAM714 planktonic 1:9
Transconjugant CFU/mL
Time (h)
0.5
1
1.5
2
5
18
B)
pAM714 biofilm 1:9
C)
pAM714 planktonic 1:1
D)
pAM714 biofilm 1:1

Figure 2

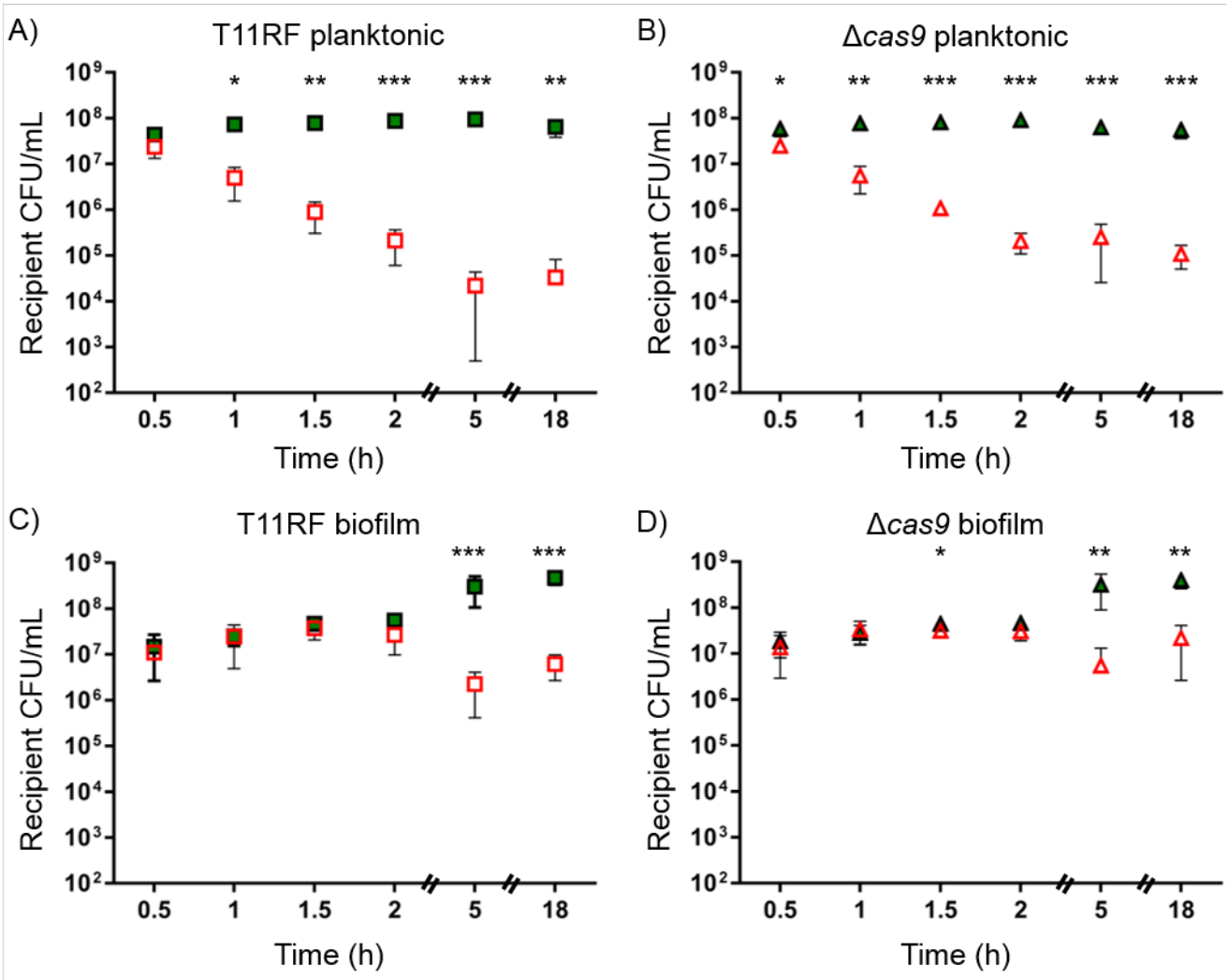
A)
T11RF planktonic
B)
Δcas9 planktonic
C)
T11RF biofilm
D)
Δcas9 biofilm
Recipient CFU/mL
Time (h)
0.5
1
1.5
2
5
18
*
**
***

Figure 3

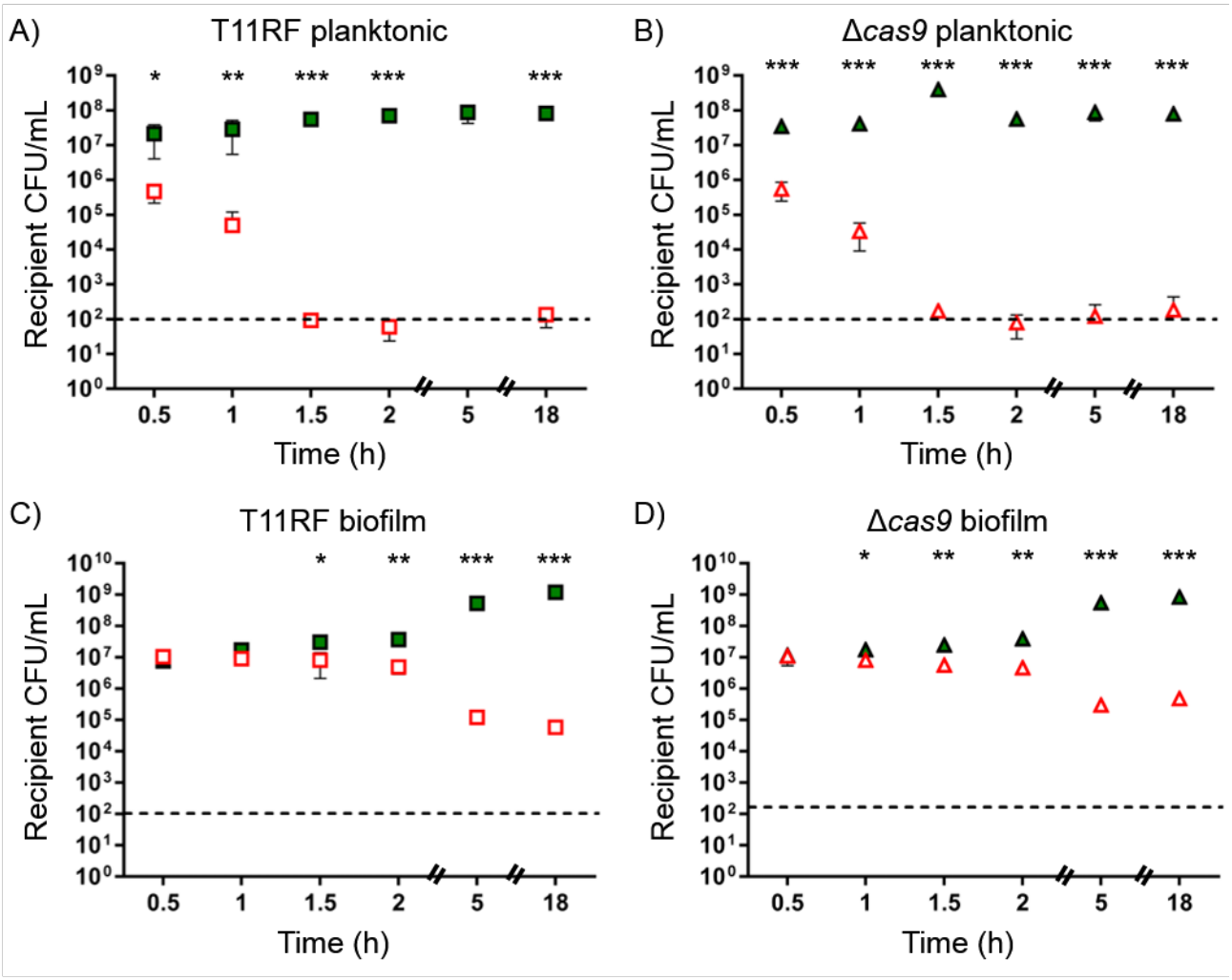
A)
T11RF planktonic
B)
Δcas9 planktonic
C)
T11RF biofilm
D)
Δcas9 biofilm
Recipient CFU/mL
Time (h)
0.5
1
1.5
2
5
18
*
**
***

Figure 4

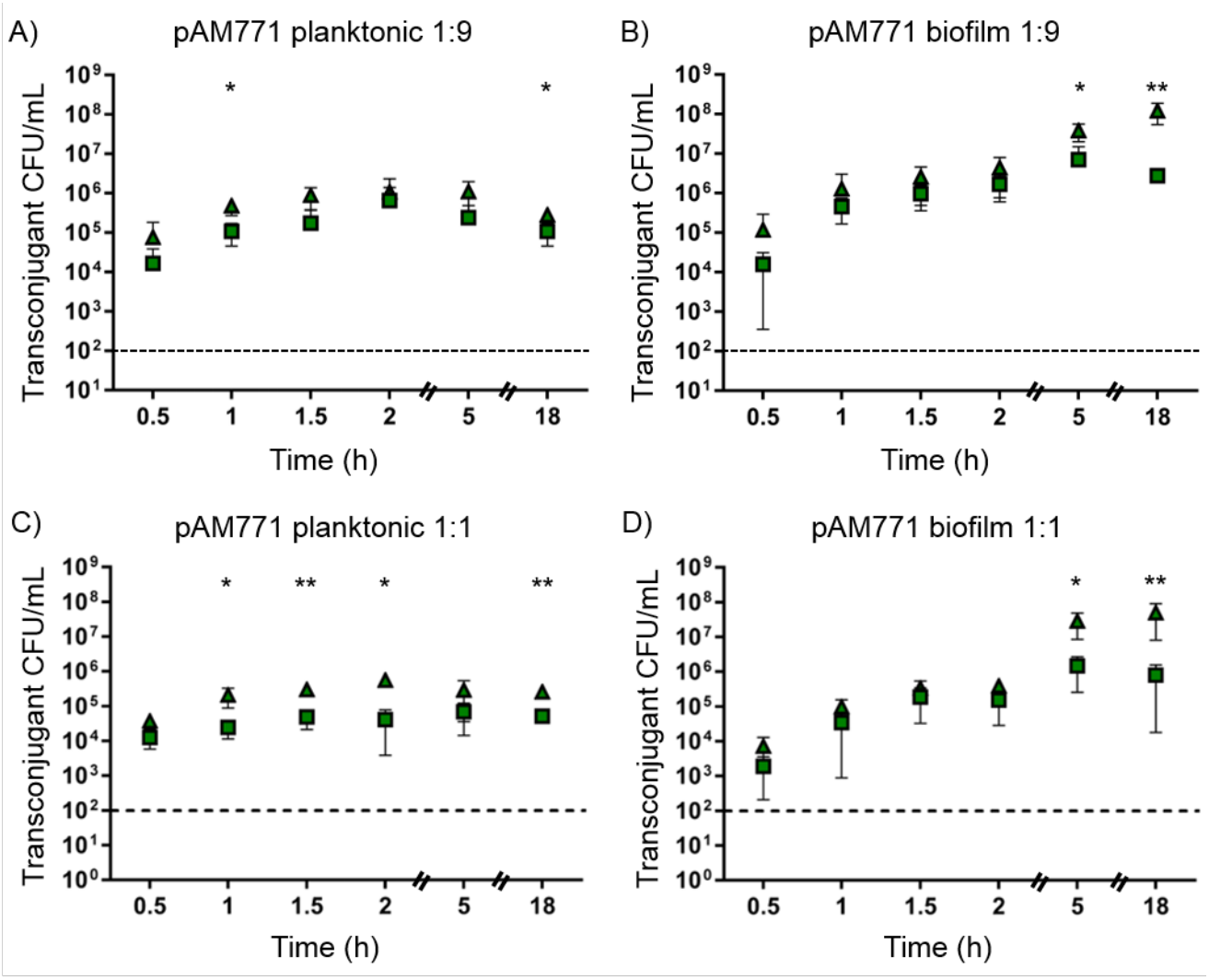
A)
pAM771 planktonic 1:9
B)
pAM771 biofilm 1:9
C)
pAM771 planktonic 1:1
D)
pAM771 biofilm 1:1
Transconjugant CFU/mL
Time (h)
0.5
1
1.5
2
5
18
*
**

Figure 5

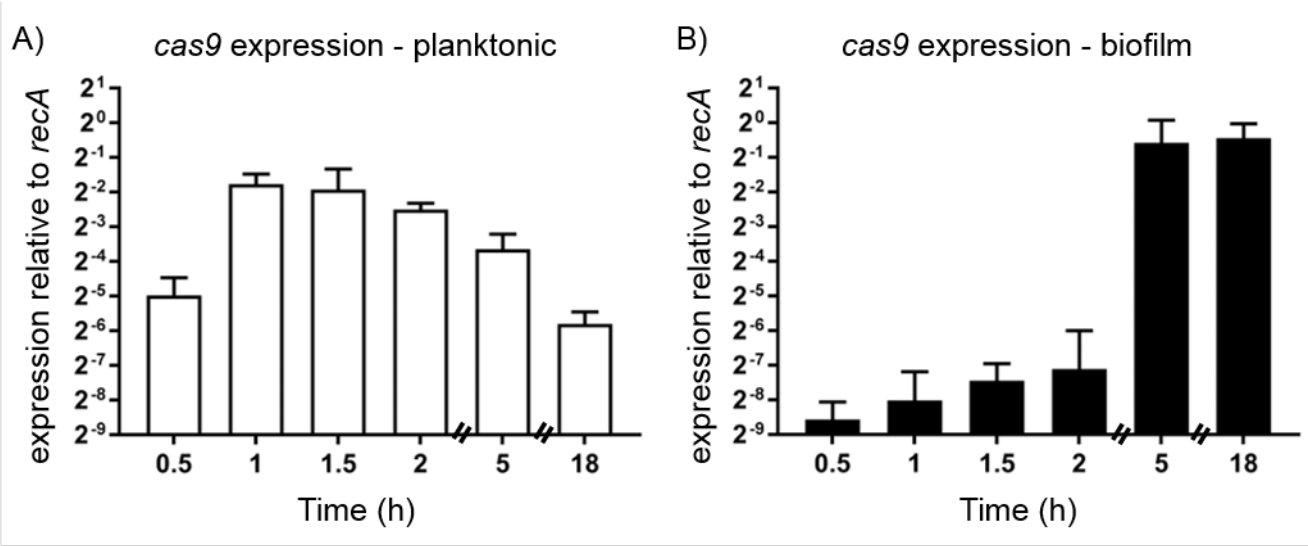
A)
cas9 expression - planktonic
expression relative to *recA*
2^{1}
2^{0}
2^{-1}
2^{-2}
2^{-3}
2^{-4}
2^{-5}
2^{-6}
2^{-7}
2^{-8}
2^{-9}
0.5
1
1.5
2
5
18
Time (h)
B)
cas9 expression - biofilm
expression relative to *recA*
2^{1}
2^{0}
2^{-1}
2^{-2}
2^{-3}
2^{-4}
2^{-5}
2^{-6}
2^{-7}
2^{-8}
2^{-9}
0.5
1
1.5
2
5
18
Time (h)

Figure 6

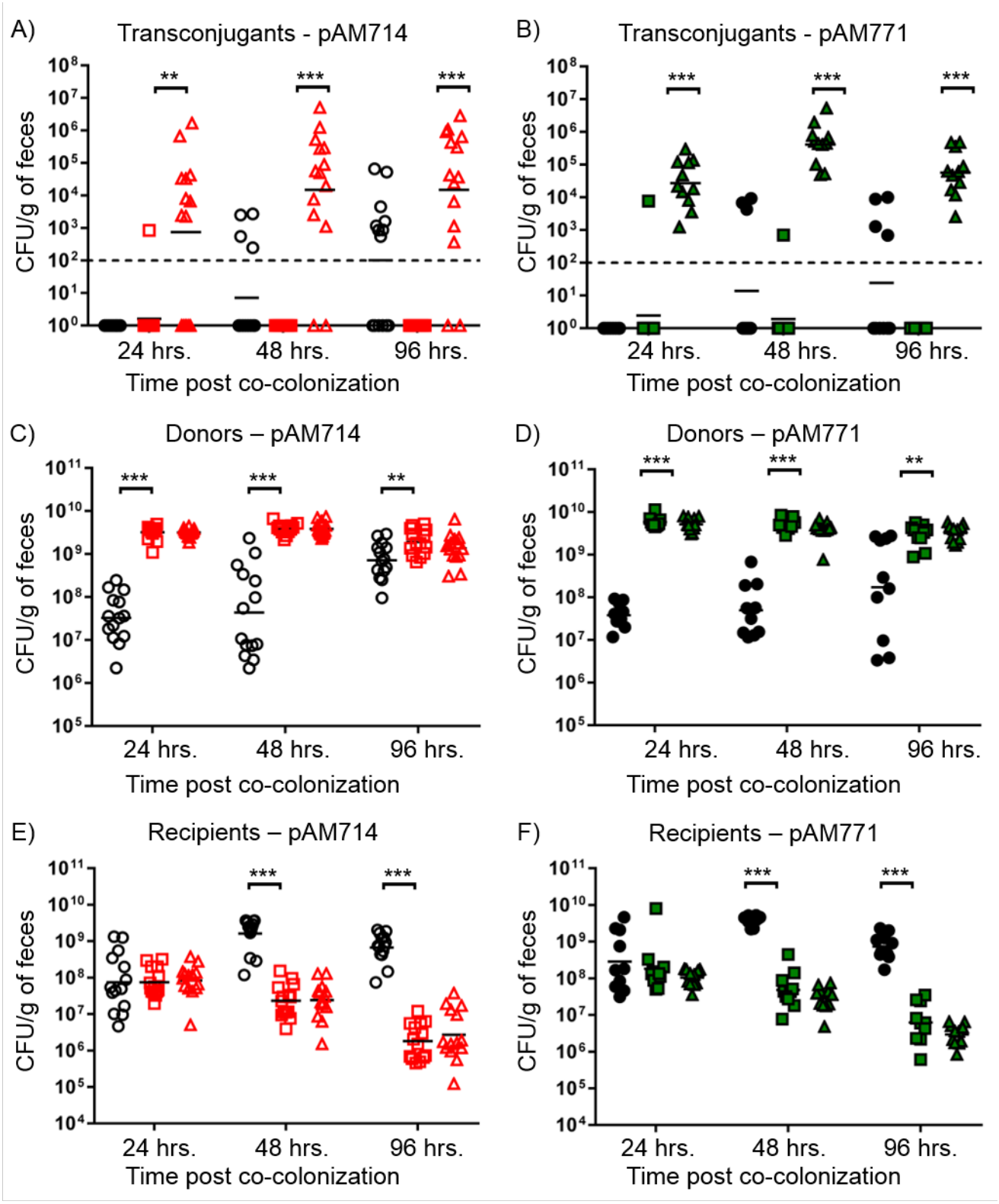
A)
Transconjugants - pAM714
B)
Transconjugants - pAM771
C)
Donors – pAM714
D)
Donors – pAM771
E)
Recipients – pAM714
F)
Recipients – pAM771
CFU/g of feces
24 hrs.
48 hrs.
96 hrs.
Time post co-colonization

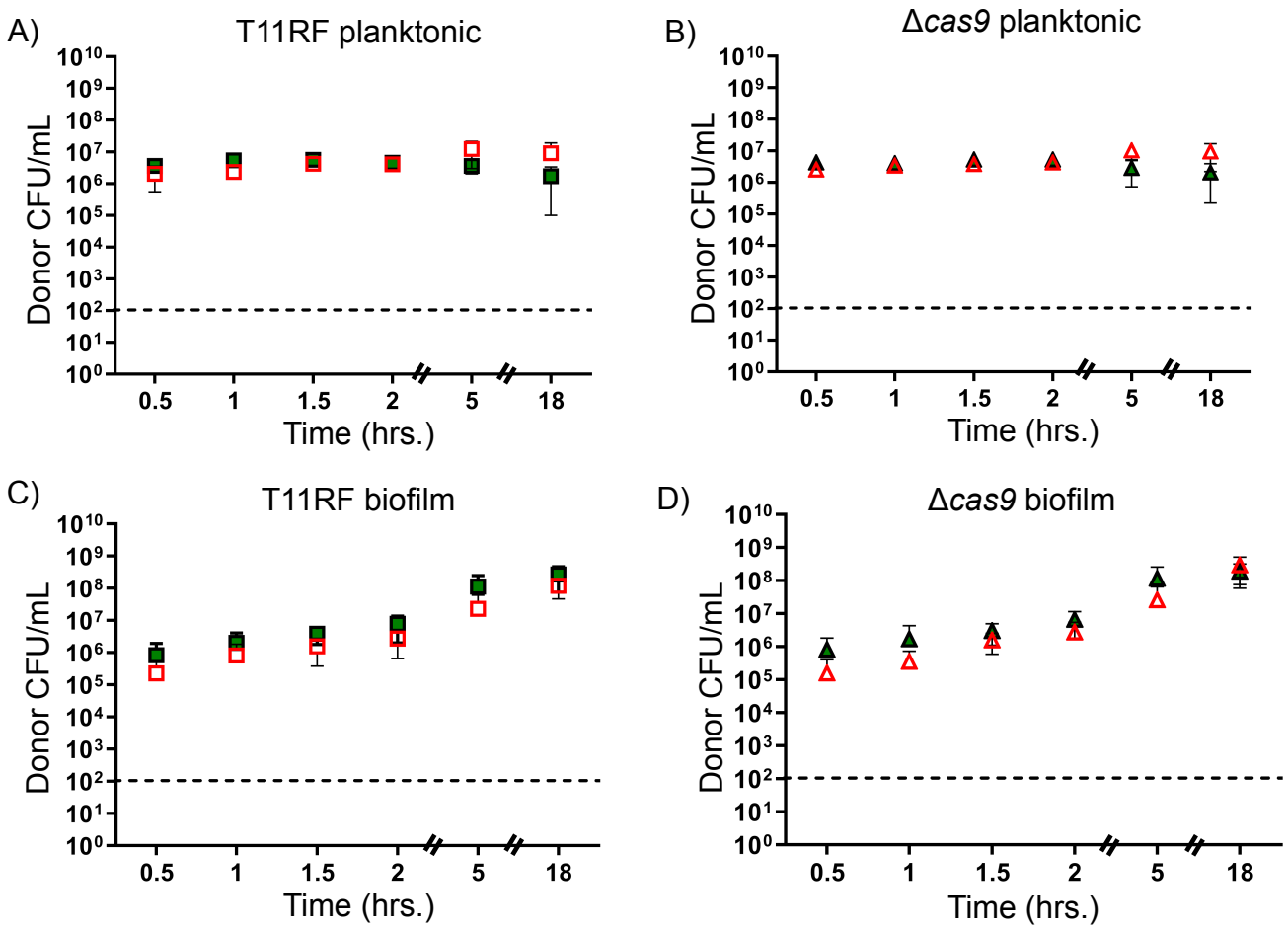

Figure S1. Donor cell densities for *in vitro* conjugations at a 1:9 donor to recipient ratio. T11RF (squares) and T11RFΔ*cas9* (triangles) donor cell densities in CFU/mL was determined for both planktonic (A and B) and biofilm (C and D) mating reactions with pAM714 (open, red symbols) and pAM771 (closed green symbols) donors. The limit of detection was 10^2 CFU/mL. Data shown are the average and standard deviation from a minimum of three independent trials for each time point for both mating conditions. Statistical significance was assessed using a two-tailed Student's t-Test; *P*-values, *<0.05, **<0.01 and ***<0.001.

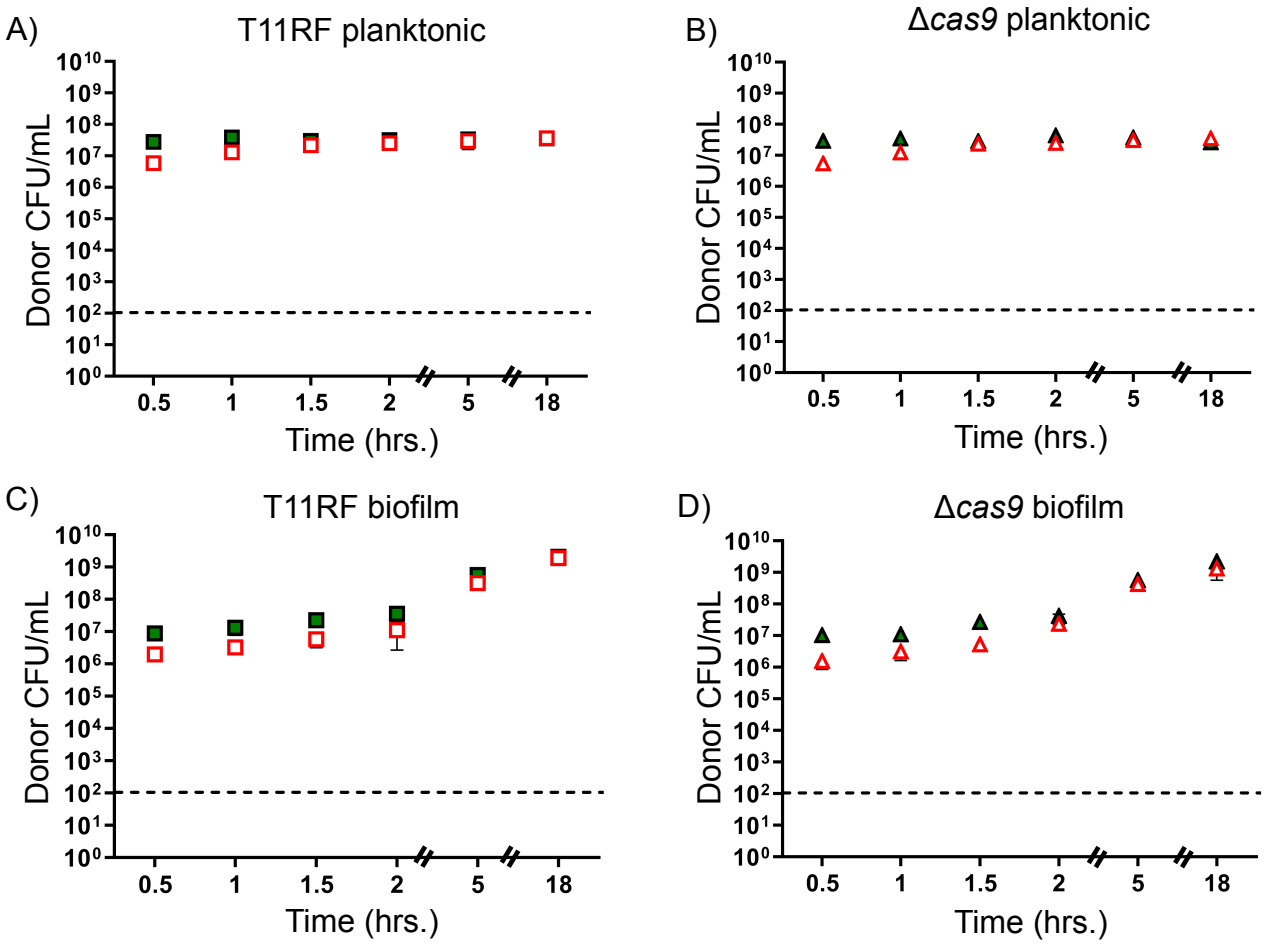

Figure S2. Donor cell densities for *in vitro* conjugations at a 1:1 donor to recipient ratio. T11RF (squares) and T11RFΔ*cas9* (triangles) donor cell densities in CFU/mL was determined for both planktonic (A and B) and biofilm (C and D) mating reactions with pAM714 (open, red symbols) and pAM771 (closed green symbols) donors. The limit of detection was 10^2 CFU/mL. Data shown are the average and standard deviation from a minimum of three independent trials for each time point for both mating conditions. Statistical significance was assessed using a two-tailed Student's t-Test; *P*-values, *<0.05, **<0.01 and ***<0.001.

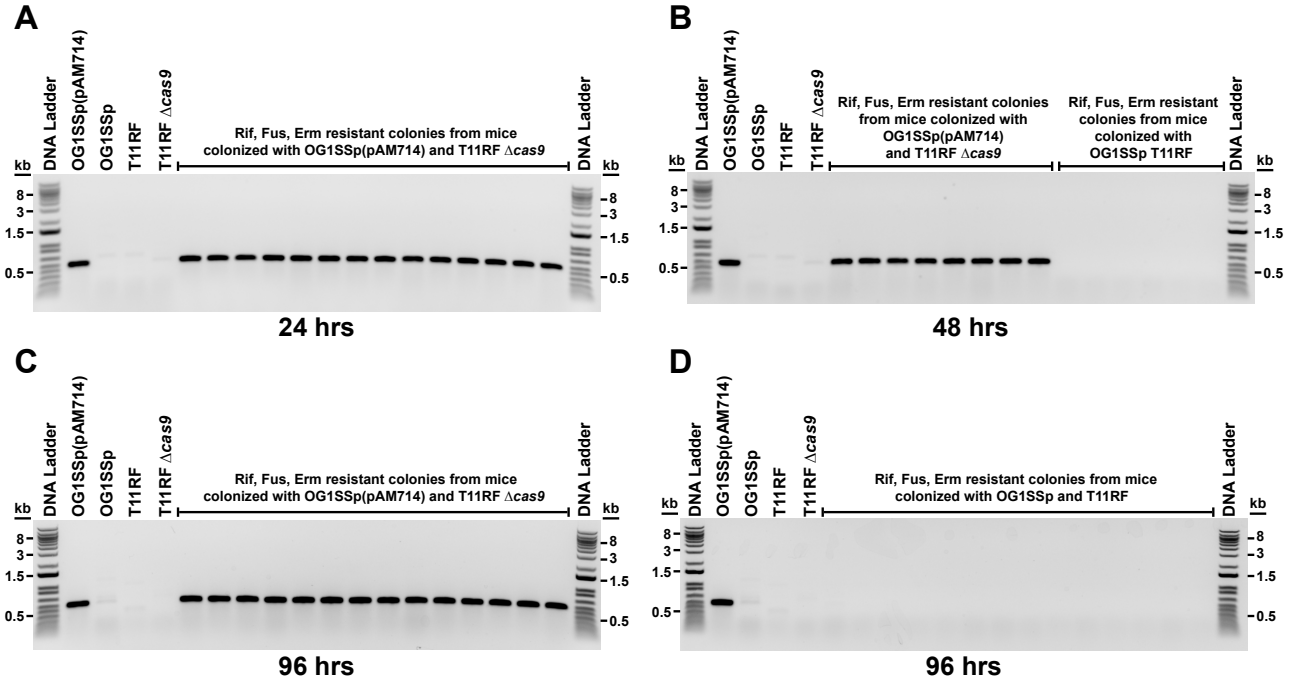

Figure S3. PCR confirms that experimental transconjugants carry pAM714 and spontaneous resistant isolates from control animals do not. Agarose gels show PCR amplification products for the *repB* gene of pAM714 at 24 (A), 48 (B) and 96 (C) hours post-colonization, and the lack of a *repB* amplification signal in isolates originating from control mice and growing on transconjugant selection agar (B and D). PCR reactions for the presence and absence of the *repB* gene using strains OG1SSp(pAM714), OG1SSp, T11RF and T11RF Δ*cas9* are included on each gel. Rif – Rifampicin, Fus – Fusidic acid, Erm – Erythromycin.

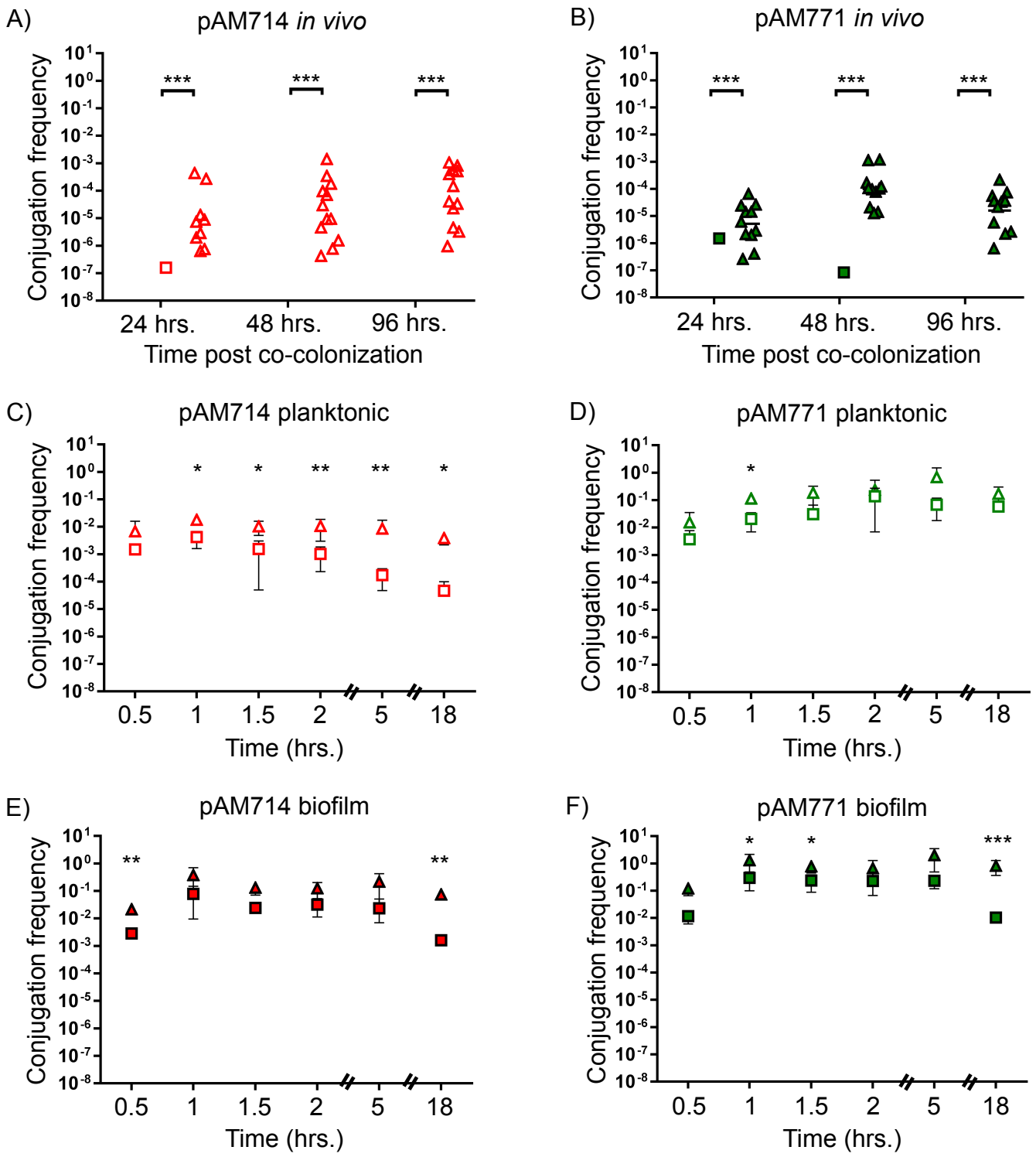

Figure S4. Frequency of conjugation *in vitro* and in the mouse intestine. Conjugation frequencies for pAM714 under mouse intestine (A), planktonic (C), and biofilm (E) settings are shown as transconjugants per donor. Conjugation frequencies for pAM771 under mouse intestine (B), planktonic (D), and biofilm (F) settings are also shown. Experiments with T11RF recipients are represented with squares; with T11RF Δ*cas9* recipients as triangles. For calculating *in vivo* conjugation frequencies, the conjugation frequency for each mouse was determined by dividing the transconjugant CFU/g by the donor CFU/g; one symbol represents one mouse on the graph. Black horizontal bars represent the geometric mean of data in each group. No symbol means that a frequency could not be calculated because one or both of the values (donor CFU/g or transconjugant CFU/g) were zero. Statistical significance was assessed using a two-tailed Student's t-Test; *P*-values, *<0.05, **<0.01 and ***<0.001.

Biofilm

T11RF monoculture biofilm time course, n=1

	t=30	t=1	t=1.5	t=2	t=5	t=18
cas9	27.21	26.60	27.52	26.73	24.94	28.83
recA	18.25	18.07	19.81	18.62	23.63	28.87

T11RF monoculture biofilm time course, n=2

	t=30	t=1	t=1.5	t=2	t=5	t=18
cas9	27.18	27.34	27.53	27.12	24.62	28.57
recA	18.46	18.87	19.77	19.84	24.57	27.98

T11RF monoculture biofilm time course, n=3

	t=30	t=1	t=1.5	t=2	t=5	t=18
cas9	26.70	25.86	26.98	27.77	25.26	29.43
recA	18.70	18.82	20.11	21.85	24.88	28.69

Planktonic

T11RF monoculture planktonic time course, n=1

	t=30	t=1	t=1.5	t=2	t=5	t=18
cas9	27.52	24.65	26.39	26.15	26.30	25.79
recA	22.20	22.68	23.98	23.45	23.14	20.40

T11RF monoculture planktonic time course, n=2

	t=30	t=1	t=1.5	t=2	t=5	t=18
cas9	26.77	25.93	26.61	26.18	28.46	27.53
recA	21.56	24.50	25.35	23.81	24.43	21.53

T11RF monoculture planktonic time course, n=3

	t=30	t=1	t=1.5	t=2	t=5	t=18
cas9	28.24	24.90	24.93	25.08	26.41	26.72
recA	23.85	23.02	22.84	22.67	22.68	20.72

Dataset S1. Ct values for RT-qPCR.